Journal of Renewable Energy and Sustainable Development (RESD)
Volume 11, Issue 1, June 2025 - ISSN 2356-8569
http://dx.doi.org/10.21622/RESD.2025.11.1.1150

Received on, 24 December 2024 Accepted on, 24 January 2025 Published on, 04 February 2025

Numerical Analysis of Baffles on Geothermal Energy in a U-shaped Heat Exchanger

Lamia Benahmed [1*], Khaled Aliane [2], Brahim Rostane [3], and Said Abboudi [4]

[1,2,3] MECACOMP Laboratory, Department of Mechanic, Faculty of Technology, University Abou Bekr Belkaid, Tlemcen, Algeria

[4] Département COMM, Carnot de Bourgogne Interdisciplinary Laboratory -UTBM, CNRS and University of Bourgogne Franche Comté (UBFC), Belfort, France

lamia.benahmed@univ-tlemcen.dz, kh_aliane@yahoo.fr, r_brahim75@yahoo.fr, said.abboudi@utbm.fr

ABSTRACT

This study investigates the enhancement of geothermal energy recovery using a vertical geothermal heat exchanger coupled with a heat pump for heating applications. The primary objective is to evaluate the impact of baffles on the thermal performance of a U-shaped heat exchanger through 3D numerical simulations. The baffles, strategically designed to modify flow dynamics, aim to optimize heat transfer and improve overall system efficiency. A comprehensive mathematical model, based on the governing equations of fluid mechanics and thermodynamics, was developed and solved using the finite volume method in Ansys CFX. Several baffle configurations were systematically analyzed, focusing on their placement (inlet and outlet tubes), geometry, and the incorporation of perforations with decreasing diameters. Simulations were performed at a Reynolds number of Re = 3600 to capture the flow behavior under specific operational conditions. The results demonstrate that the optimal configuration featuring baffles placed on the outlet tube with perforations of decreasing diameters significantly enhances thermal performance. Specifically, this configuration improves the heat transfer coefficient by 25% and increases the overall system efficiency by 18% compared to a baseline design without baffles. Additionally, the pressure drop was maintained within acceptable limits, increasing by only 12%, which ensures minimal energy losses. These findings provide valuable insights for the design of advanced heat exchangers in geothermal systems, offering a pathway to more sustainable and efficient energy solutions. The study underscores the importance of innovative design modifications, such as baffle integration, in optimizing renewable energy technologies.

Index-words: *Geothermal energy, Heat transfer, U-shaped exchanger, Baffles, Turbulence model, ANSYS -CFX.*

Nomenclature	
Pr	Pranth Number
U	Velocity, m/s
Ub	Mean bulk velocity, m/s
ui'	Time-averaged velocity in x_i direction, m/s
uj'	Time-averaged velocity in x_j direction, m/s
$ui' uj'$	Reynolds stresses, i, j = x, y, z m^2/s^2
u,v,w	Next speed components (x, y, z), m/s
P	Pressure, Pa
T	Temperature, K
P_k	Rate of Production
d_0	Diameter of baffles, mm
D_R	Baffle thickness, mm
L	Depth, mm
D	Distance, mm
d	Internal pipe diameter, mm
t	Pipe thickness, mm
Re	Reynolds number
k	kinetic energy of turbulence, m^2/s^2
Greek Symbols	
ϕ	Physical size
μ	Dynamic viscosity, Pa.s
μt	Turbulent kinematic eddy viscosity, Pa.s
σ_k	Prandtl number of turbulent kinetic energy
σ_ε	Dissipation energy
ε	Turbulent dissipation, m^2/s^3
ρ	Density, kg/m^3
ω	Specific dissipation, 1/s

Volume 11, Issue 1, June 2025 - ISSN 2356-8569
http://dx.doi.org/10.21622/RESD.2025.11.1.1150

I. INTRODUCTION

Among renewable energy sources, geothermal energy stands out as a reliable and sustainable option that harnesses the natural heat from within the Earth. This heat, generated by the decay of radioactive elements and thermal processes at the core of the planet, can be accessed in various forms, such as hot water, steam, and heated rocks. It is used to produce electricity, heat buildings, and power industrial systems, providing a sustainable energy solution with a low carbon footprint. Due to its constant availability, geothermal energy is a promising alternative to address global energy challenges while preserving the environment.

Geothermal energy is the science that studies the internal thermal phenomena of the terrestrial globe and the technique that aims to exploit them [1]. The principle consists of exploiting the geothermal energy contained in the ground via a heat exchanger and taking advantage of the temperature difference between that of the environment and the ground at a defined depth to heat in winter or cool in summer [2].

Recently, various studies have been carried out on a Ground Source Heat Pump and geothermal heat-exchanger system through numerical investigations [3-7].

There are several technologies to ensure heat exchange between the buildings and the basement [8-10]. For example, we can mention heat pump systems, equipped with vertical or horizontal geothermal collectors. Geothermal heat pumps are a renewable energy technology that have garnered significant attention and have been utilized for both heating and cooling purposes [11-14].

Several studies have been done to examine the effectiveness of geothermal heat pump systems [15-17]. Additionally, the authors [18-20] demonstrated that the subterranean heat exchanger system could lower the borehole depth.

Matthew and colleagues [21] conducted an experimental study on the effectiveness of a BHE vertical in the form of a U, where temperature changes and the thermal equilibrium of the system were simulated and numerically analyzed. These findings indicated that in order for the geothermal heat pump system to achieve higher output and greater energy storage, the geothermal source could be used as a thermal source or pump. The cooling capabilities of the geothermal heat pump system installed in a South Korean school building were investigated by Hwang et al. [22]. They talked about how well the system worked and how the outside temperature affected everything. In Denizli, Turkey, Karabacak et al.'s [23] experimental study examined the cooling capabilities of the geothermal heat pump system. They successfully demonstrated how the weathering information, such as solar radiation, wind speed, relative humidity, and outside temperature, relates to the coefficients of operation of the geothermal heat pump. To evaluate Turkey's cold weather, Ozyurt et al. [24] conducted an experimental investigation into the performance of vertical geothermal heat pumps. The results included the calculation of the coefficients of performance for both the heat pump and the system. Michopoulos et al. [25,26] investigated the operation of a heating and cooling system that was put in place in Greece. Recent studies have further expanded our understanding of geothermal heat pump systems in diverse environments. For example, Kolo et al. [27] provides a comprehensive review of DBHEs, highlighting advancements in subsurface modeling and their applications in various geological settings. Similarly, Ma et al. [28] investigated the effects of boundary conditions on the performance of deep-buried ground heat exchangers, emphasizing the importance of accurate modeling for optimizing energy utilization. In regions with extreme climates, such as severe cold areas, Guo et al. [29] demonstrated the heating potential and sustainability of medium-deep borehole heat exchangers, offering insights into their practical implementation. Furthermore, Guo et al. [30] explored the conversion of end-of-life oil and gas wells into geothermal wells, comparing direct and reverse circulation methods to assess heat energy productivity.

These studies collectively underscore the versatility and efficiency of geothermal heat pump systems across different climates and applications. However, further research is needed to explore the long-term performance and scalability of these systems, particularly in regions with extreme weather conditions or limited geothermal resources.

Akbar et al. [31] quantitatively explored the unstable flow of a high enthalpy fluid in a geothermal BHE. They used the finite element approach to solve the governing equations and looked into significant physical phenomena along the wells, such as phase change, compressibility, and thermal contact.

Volume 11, Issue 1, June 2025 - ISSN 2356-8569
http://dx.doi.org/10.21622/RESD.2025.11.1.1150

The heat transmission in a U-shaped BHE was simulated and analytically examined by Bni Lam et al. [32]. They investigated the impact of friction at various flow speeds and viscosities while discretizing in the time domain. L. Benahmed et al. [33,34] studied the influence of the inclined form of the two upper peaks of a rectangular cube and the insertion of hollow in the cube to visualize the turbulent flow around an obstacle. A three-dimensional configuration was carried out using the ANSYS CFX calculation code. Turbulence models have been used to study the flow characteristics around the inclined and perfored cube. Rostane et al. [35,36] analyzed the influence of the perforation volume of the cubes is studied and compared with the case of obstacles without holes for a constant heat flux subjected to the solid part.

The aim of this work is to present a 3D numerical study to evaluate the effects of baffles on the performance of a U-shaped heat exchanger.

Our ultimate goal is to improve heat transfer to ensure optimum heating performance. Different models of the insertion of baffles in the U pipe (simple U pipe, U pipe with baffles in the pipe in, U pipe with baffles in the pipe out, U pipe with baffles in the pipe in and pipe out) were processed to execute this.

In the following sections, the methodology used for the numerical simulations is presented, detailing the setup of the U-shaped heat exchanger models and the baffle configurations. The results section provides an analysis of the heat transfer performance for each baffle model, comparing temperature profiles and flow characteristics. Finally, the conclusion summarizes the key findings and suggests potential improvements for further research in optimizing heat exchanger designs for better thermal efficiency.

II. MATHEMATICAL MODEL

Average equations of conservation of mass, momentum, energy, and Reynolds are:

- The mass conservation equation

$$\frac{\partial \rho}{\partial t} + \frac{\partial (\rho U_i)}{\partial x_i} = 0 \quad (1)$$

- Momentum Conservation

$$\frac{\partial U_i}{\partial t} + U_j \frac{\partial U_i}{\partial x_j} = -\frac{1}{\rho}\frac{\partial P}{\partial x_i} + \upsilon \frac{\partial^2 U_i}{\partial x_j \partial x_j} \quad (2)$$

- Energy Equations

$$\frac{\partial \overline{T}}{\partial t} + \overline{U}_j \frac{\partial \overline{T}}{\partial x_j} = \frac{\partial}{\partial x_j}\left[\left(\frac{\mu}{\Pr} + \frac{\mu_t}{\Pr_t}\right)\frac{\partial \overline{T}}{\partial x_j}\right] + \frac{1}{\rho C_P}\Phi \quad (3)$$

- Reynolds Equations

$$\rho \frac{\partial \overline{U_i}}{\partial t} + \rho \overline{U}_j \frac{\partial \overline{U_i}}{\partial x_j} = -\frac{\partial \overline{P}}{\partial x_i} + \frac{\partial}{\partial x_j}\left(\mu \frac{\partial \overline{U_i}}{\partial x_j} - \rho \overline{u'_i u'_j}\right) \quad (4)$$

The K-ω SST (Shear Stress Transport) model of Stephan [37] was the turbulence model used in this study. It is derived from the Standard k-ω model [38] and combines the k-ε model [39] and all of its types such as the free flow away from the wall with the robustness and accuracy of the formulation of the k-ω model in the near-wall region. The definition of turbulent viscosity is modified to account for the transport of turbulent shear stresses.

The two-equation model is formulated as follows:

$$\rho \frac{\partial k}{\partial t} + \rho \overline{U}_j \frac{\partial k}{\partial x_j} = \tilde{P}_k - \rho C_\mu \omega k + \frac{\partial}{\partial x_j}\left[(\mu + \mu_t/\sigma_k)\frac{\partial k}{\partial x_j}\right] \quad (5)$$

Specific dissipation rate:

$$\rho \frac{\partial \omega}{\partial t} + \rho \overline{U}_j \frac{\partial \omega}{\partial x_i} = 2\alpha\rho S_{ij} S_{ij} - \beta\rho\omega^2 + \frac{\partial}{\partial x_j}\left[(\mu_t + \sigma_\omega \mu_t)\frac{\partial \omega}{\partial x_j}\right] + 2(1 - F_1)\rho\sigma_{\omega 2}\frac{1}{\omega}\frac{\partial k}{\partial x_j}.\frac{\partial \omega}{\partial x_j} \quad (6)$$

The blend function F_1 is defined by:

$$F_1 = \tanh\left\{\left\{\min\left[\max\left(\frac{\sqrt{k}}{C_\mu \omega L}, \frac{500\upsilon}{L^2\omega}\right)\frac{4\rho\sigma_{\omega 2} k}{CD_{k\omega} L^2}\right]\right\}^4\right\} \quad (7)$$

Here y is the distance to the nearest wall. In the near-wall region, $F1$=1, while it goes to zero in the outer region $CDk\omega$ is given as:

$$CD_{k\omega} = \max\left(2\rho\sigma_{\omega 2}\frac{1}{\omega}\frac{\partial k}{\partial x_j}.\frac{\partial \omega}{\partial x_j}, 10^{-10}\right) \quad (8)$$

Eddy viscosity is given by

$$\upsilon_t = \frac{\alpha_1 k}{\max\left(\alpha_1 \omega, \sqrt{2} S_{ij} F_2\right)} \quad (9)$$

Volume 11, Issue 1, June 2025 - ISSN 2356-8569
http://dx.doi.org/10.21622/RESD.2025.11.1.1150

The second blending function is defined by:

$$F_2 = \tanh\left[\left[\max\left(\frac{2\sqrt{k}}{C_\mu \omega L}, \frac{500\,\upsilon}{L\,\omega^2}\right)\right]^2\right] \quad (10)$$

To prevent the accumulation of turbulence stagnation regions, limited production was used:

$$\tilde{P}_k = \min\left(P_k, 10 \cdot C_\mu \rho k \omega\right) \quad (11)$$

$$P_k = \mu_t \frac{\partial U_i}{\partial x_j}\left(\frac{\partial U_i}{\partial x_j} + \frac{\partial U_j}{\partial x_i}\right) \quad (12)$$

The model constants are calculated using the mixing function F1:

$$\phi = F_1 \phi_1 + (1 - F_1)\phi_2 \quad (13)$$

The values of the model constants are:

C_μ =0.09, α_1 =5/9, α_2 =0.44, β_2 =0.0828, σ_{k1} =0.85, σ_{k2} =1.0, $\sigma_{\omega 1}$=0.5, $\sigma_{\omega 2}$ =0.856

The k-ω SST model is mainly recommended for applications such as fluids experiencing abrupt stress changes, flowing through curved surfaces or boundary layer separation cases, so it is the perfect model for our simulation.

III. MODEL DESCRIPTION AND COMPUTATIONAL DOMAIN

A. Geometry and Computational Domain

The geometry of the problem is presented in Fig.1. It is a U-shaped geothermal exchanger (soil/water exchanger). The dimensions of the exchanger are shown in Table I.

A well-refined mesh must be generated to improve the accuracy of the outcomes. Using the calculation code ANSYS CFX, we chose to use a structured tetrahedral model in our study. The mesh grid in use is displayed in Fig. 3.

TABLE I. U TUBE SIZING

Features	Symbol	Size (mm)
Pipe deepness	L	1000
Internal pipe diameter	D	26
Pipe thickness	T	2.9
Distance from the center of the tow pipes	D	78

TABLE II. THE GEOMETRIC PARAMETERS OF THE BAFFLES

Numbers of baffles	P (mm)	d (mm)	d_0 (mm)	D_r
1	125	26	23	1.3
2		26	20	1.3
3		26	17	1.3
4		26	14	1.3
5		26	11	1.3

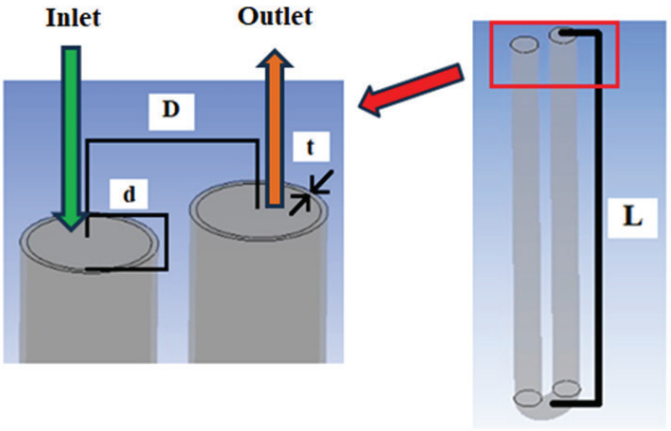

Cas (a)

Fig. 1. Geometry of U-shaped heat exchanger (3D view)

To improve heat transfer in the exchanger, ring-shaped baffles are used. The length of the test section is half of the total length of the pipe and is located one quarter of the length of the pipe from its beginning (Figure.2). Table II represents the geometric parameters of the rings, such as pitch (P), thickness (Dr), and diameters (d).

Volume 11, Issue 1, June 2025 - ISSN 2356-8569
http://dx.doi.org/10.21622/RESD.2025.11.1.1150

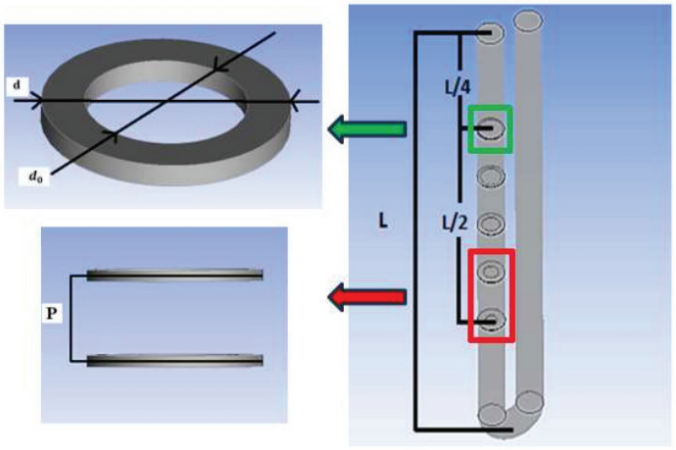

Cas (b)

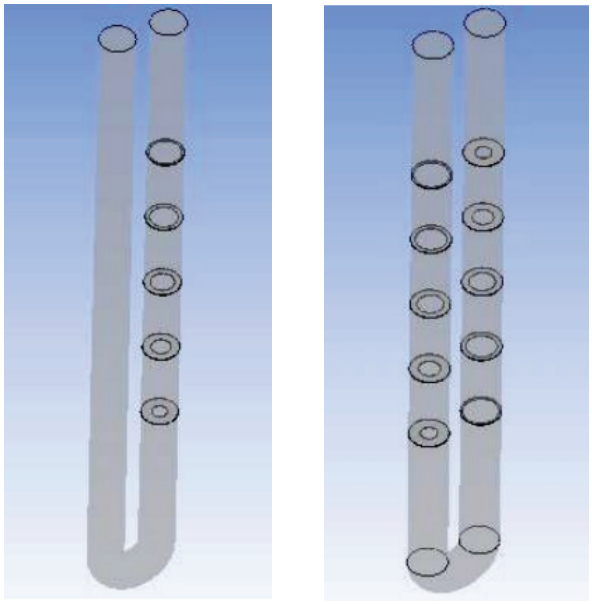

Cas (c) Cas (d)

Fig. 2. The geometry of the different cases studied

B. Boundary Conditions

The turbulence k-ω SST model was selected to more accurately examine the situation since the flow is turbulent. Equations were solved using the following elements, per the previously chosen models: The Reynolds numbers Re=3600, ($Re=U_0.d/v$) and the internal pipe diameter (d) are correlated with the incoming flow velocity U_0. T = 278 K is the entrance temperature, and Pout = 0 is the outlet pressure. The boundary conditions of the problem are presented in Table III.

The tetrahedral structured with O-grid meshes is used to solve the previously mentioned equations. This mesh structure has been refined near the solid walls for greater accuracy. The continuity, momentum, and energy equations are solved using the finite volume method implemented in the ANSYS CFX code. To handle the convection terms, the second-order Upwind scheme is applied.

TABLE III. BOUNDARY CONDITIONS

Geometry	U tube
Flow regime	Turbulent
Fluid type	Water
Turbulence model	K−ω SST
Fluid velocity [m/s]	0.72
Inlet fluid temperature [K]	275
Wall temperature [K]	283
Relative Pressure [Pa]	0

IV. RESULTS AND DISCUSSION

A. Grid Independency Study

Mesh selection is a crucial step in numerical simulations, as it has a strong influence on the accuracy of results and computation time. To ensure that the results of our study are mesh-independent, we ran simulations with three different configurations (Table IV): 738387, 537717, and 396434 tetrahedral elements.

To assess the mesh-independence of the results, we compared the outlet temperatures in the pipe out obtained for each configuration (Fig. 4). The results show relatively small differences between the three meshes, suggesting convergence of the solutions. The mesh size of (537717) was chosen as the best solution between precision and calculation time.

TABLE IV. DIFFERENT MESHING SIZES

Configuration 1	Configuration 2	Configuration 3
396434	537717	738387

Volume 11, Issue 1, June 2025 - ISSN 2356-8569
http://dx.doi.org/10.21622/RESD.2025.11.1.1150

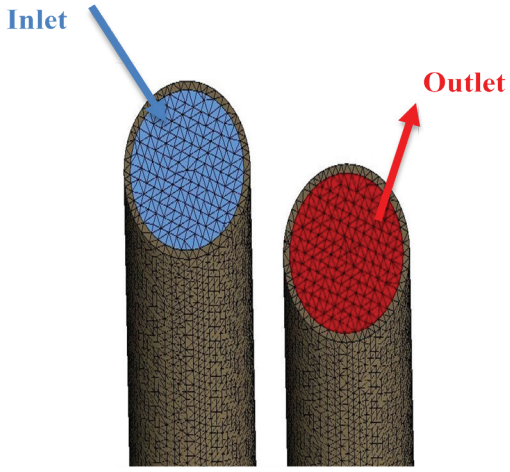

Fig. 3. The grid mesh of the configuration

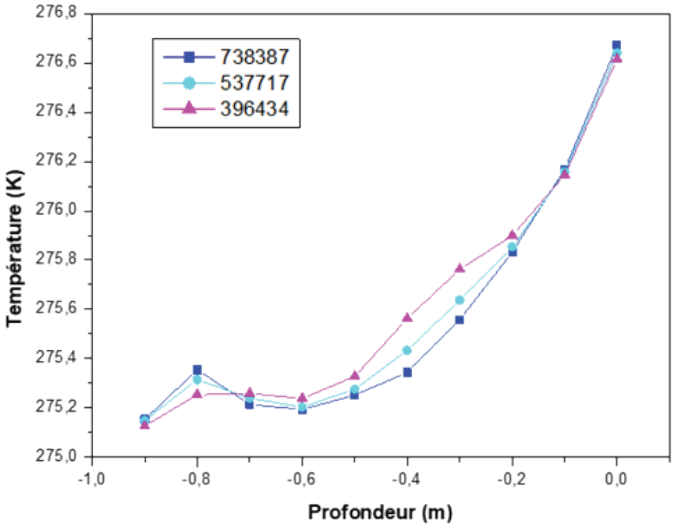

Fig. 4. The grid sensitivity

B. Code Validation

Before considering the effect of inserting baffles into a U-tube on heat transfer, we first validated our numerical results with those obtained from the numerical work of Jalilia et al. [40] and El Khoury [41] for a U-tube with a height of 1000 mm and an internal diameter of 26 mm. A flow velocity of 0.01 m/s is applied at the tube inlet, corresponding to a Reynolds number of 50.

Fig. 5 presented the profiles of the temperatures at the outlet of the pipe. These temperature profiles show, compared to those obtained numerically by Jalilia et al. [40] and El Khoury [41], an almost perfect coincidence and a good agreement between both approaches.

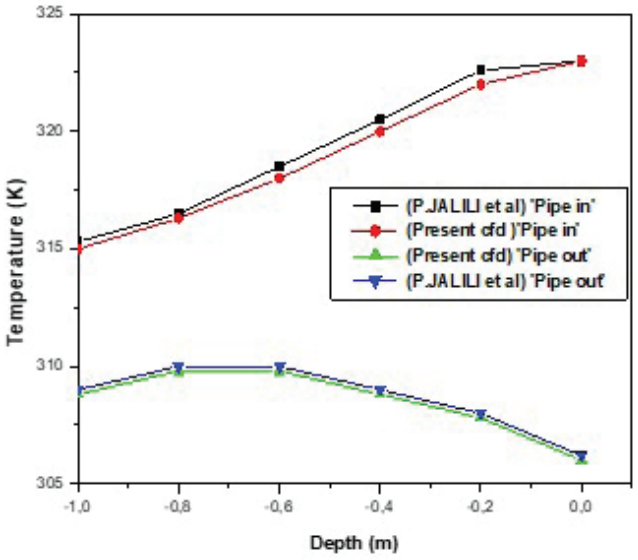

Fig. 5. Validation of the temperature profiles at the pipe out and pipe in

C. Variation of Velocity, Temperarure, Turbulence Kinetic Energy and 3D Streamlines

The study of the impact of the insertion of baffles in the middle of a pipe in U has been examined. A three-dimensional study was carried out using the ANSYS CFX calculation code. Turbulence model K-ω SST has been employed to examine the features of the different sections of baffles at Reynolds number Re=3600. The contours of temperature, velocity, turbulence kinetic energy, 3D time-averaged streamlines, temperature and velocity profiles, trace-lines around the baffles have been presented.

In cases (b) and (d), after passing through the baffles, the velocity of the fluid increases relative to its initial value. This can be attributed to the fact that baffles act to constrict the flow path, causing a reduction in the cross-sectional area available for flow. According to the continuity equation (A1v1 = A2v2, where A is the cross-sectional area and v is the velocity), when the flow area is reduced, the velocity must increase to maintain the mass flow rate. This is a typical behavior observed in pipe flow through constrictions or nozzles, and it leads to an acceleration of the flow as it exits the baffles.

However, in case (c), where the baffle perforations are increased, the velocity of the fluid decreases. This happens because a larger opening increases the flow area, reducing the fluid velocity in line with the continuity equation. Essentially, the fluid is able to

Volume 11, Issue 1, June 2025 - ISSN 2356-8569
http://dx.doi.org/10.21622/RESD.2025.11.1.1150

spread out more, leading to a lower velocity as the cross-sectional area increases. Additionally, larger perforations may result in less disruption of the flow, causing less turbulence and lower velocity at the exit of the baffles.

This interplay between the flow area, velocity, and turbulence is critical in understanding how baffles impact heat transfer and flow behavior.

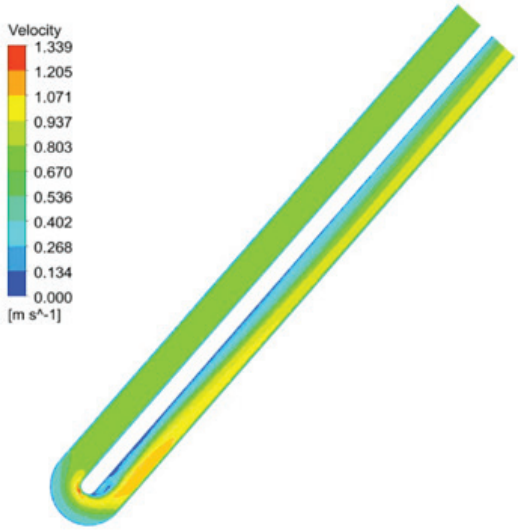

Cas (a)

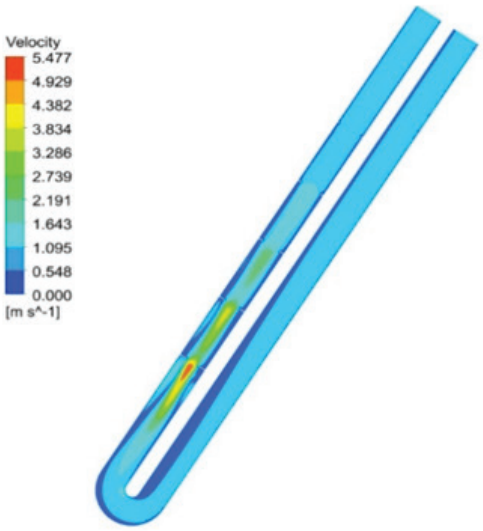

Cas (b)

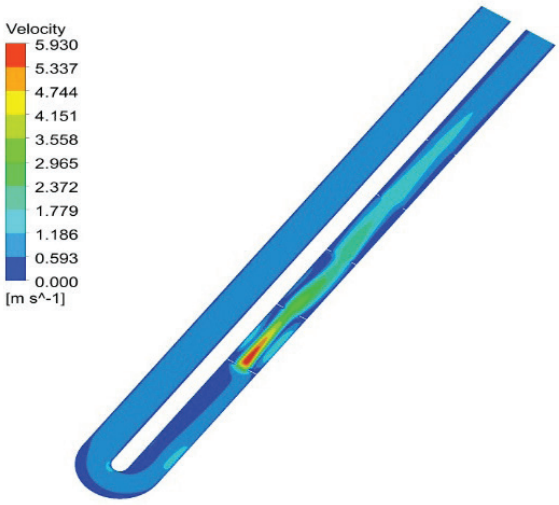

Cas (c)

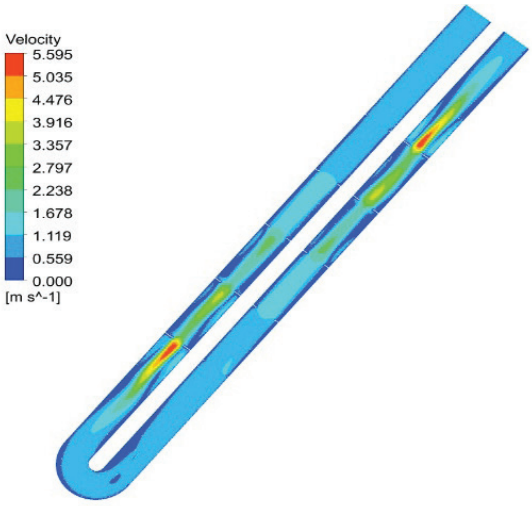

Cas (d)

Fig. 6. Contours of velocity for different cases

The numerical results shown in Fig. 7 demonstrate that as the fluid velocity increases, so does the wall temperature, directly impacting the temperature at the exchanger outlet. This is because the friction between the fluid and the walls converts kinetic energy into thermal energy, raising the temperature of the fluid. The increase in fluid velocity improves convective heat transfer, which leads to higher temperatures at the exchanger outlet.

Volume 11, Issue 1, June 2025 - ISSN 2356-8569
http://dx.doi.org/10.21622/RESD.2025.11.1.1150

- **Influence of Baffles on Heat Transfer:**

The baffles inserted into the heat exchanger play a crucial role in increasing turbulence in the fluid flow. When the fluid hits the baffles, the flow becomes disrupted, which results in a more uniform heat transfer as the fluid experiences different temperature zones. The turbulent flow caused by the baffles increases the heat exchange rate by enhancing the interaction between the fluid and the tube walls. This disruption effectively breaks down boundary layers near the walls, allowing for better heat conduction from the fluid to the tube walls.

- **Influence of Annular Sections with Decreasing Diameters:**

Additionally, the effect of annular sections with decreasing diameters is particularly noteworthy. In cases where the diameter of the baffle openings reduces towards the outlet (case d), the fluid velocity increases further, leading to higher heat transfer rates. This is consistent with the principle that a reduction in cross-sectional area forces the fluid to speed up to maintain mass flow continuity. The faster flow, combined with the smaller openings, enhances turbulence, which facilitates more effective heat exchange.

- **Impact on Geothermal Heat Pump Efficiency:**

The increase in temperature at the exchanger outlet, driven by the higher fluid velocity and the turbulent flow from the baffles, directly affects the work done by the geothermal heat pump condenser. As the temperature at the outlet rises, the geothermal system becomes more efficient, requiring less work from the condenser. The use of annular baffles with decreasing diameters further enhances this effect by increasing the flow velocity and turbulence, improving the overall energy efficiency of the system. The numerical results illustrated in Fig. 7. indicate that as the fluid velocity increases, so does the wall temperature. This increase causes the temperature at the exchanger outlet to rise.

The presence of the baffles increases the turbulence of the fluid, which leads to an increase in heat exchange and therefore an increase in the outlet temperature, which minimizes the work of the condenser and therefore improves the efficiency of the geothermal heat pump.

Volume 11, Issue 1, June 2025 - ISSN 2356-8569
http://dx.doi.org/10.21622/RESD.2025.11.1.1150

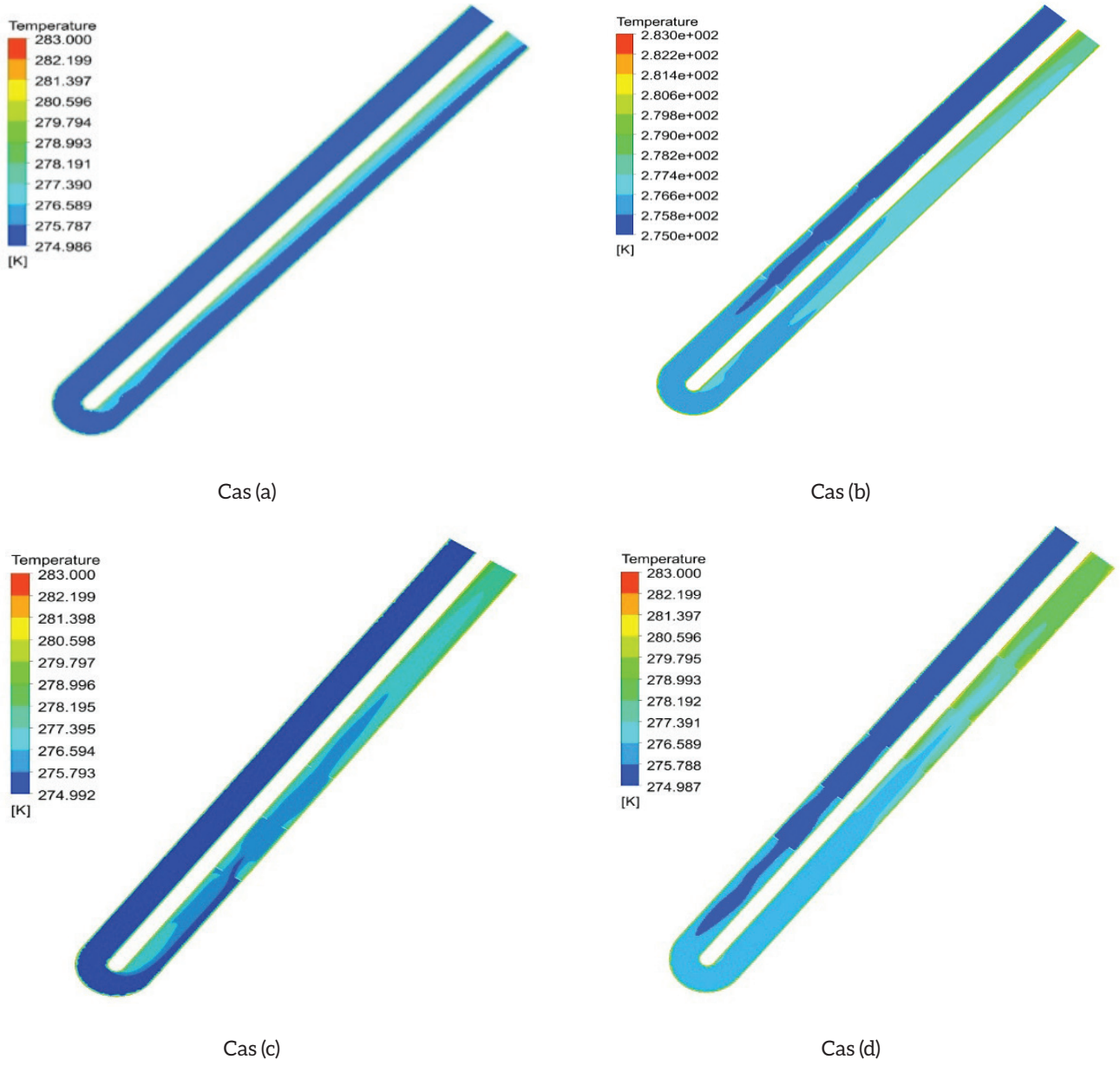

Fig. 7. Contours of temperature for different cases

In Fig. 8, the data reveal key insights into how the fluid kinetic energy behaves at different points in the U-shaped heat exchanger, with noticeable variations depending on the case and the flow conditions.

1. ***Case (a):*** In this scenario, there is a noticeable increase in kinetic energy in areas where the fluid flow path is sharply curved. When the flow trajectory changes direction abruptly, it causes the fluid particles to accelerate and decelerate. These changes lead to the conversion of thermal energy into kinetic energy, especially in regions with strong curvature. The sudden redirection of the fluid flow results in higher turbulence, which in turn increases the kinetic energy, as seen in the data. This is consistent with studies on flow turbulence, which have shown that sharp bends in flow paths cause fluctuations in both velocity and kinetic energy (Benahmed et al., 2020).

2. ***Cases (b), (c), and (d):*** For these cases, the turbulent kinetic energy peaks where the fluid velocity is at its maximum. This is a typical feature of turbulent flow dynamics. As the fluid accelerates, particularly after passing through the baffles, the velocity increases and the turbulent kinetic energy also reaches its highest values in those regions. This aligns with established fluid dynamics principles where turbulence intensifies when the flow speed increases, particularly in constrained or highly turbulent regions. In these cases, the

Volume 11, Issue 1, June 2025 - ISSN 2356-8569
http://dx.doi.org/10.21622/RESD.2025.11.1.1150

turbulent energy is directly tied to the fluid velocity, with peaks occurring where the flow experiences the most significant acceleration.

3. ***Fluctuations and Minimum Kinetic Energy:*** In areas where the fluid velocity is less accelerated, fluctuations in kinetic energy become evident. These fluctuations are due to the varying degrees of turbulence. As the fluid passes through regions with lower acceleration or deceleration, such as after the baffles or where the flow area widens, the kinetic energy reaches a minimum. This behavior reflects the dissipation of turbulent kinetic energy when the flow stabilizes and the fluid velocity decreases. The data suggests that the energy fluctuations are linked to the instability in the flow, which transitions from a high-energy state to a more stable, lower-energy state as it progresses through the system.

These observations underscore the dynamic interaction between flow velocity and kinetic energy in a heat exchanger system with baffles. The variations in kinetic energy are crucial for understanding how turbulence and flow acceleration or deceleration impact the overall performance of the heat exchanger, particularly in terms of heat transfer efficiency.

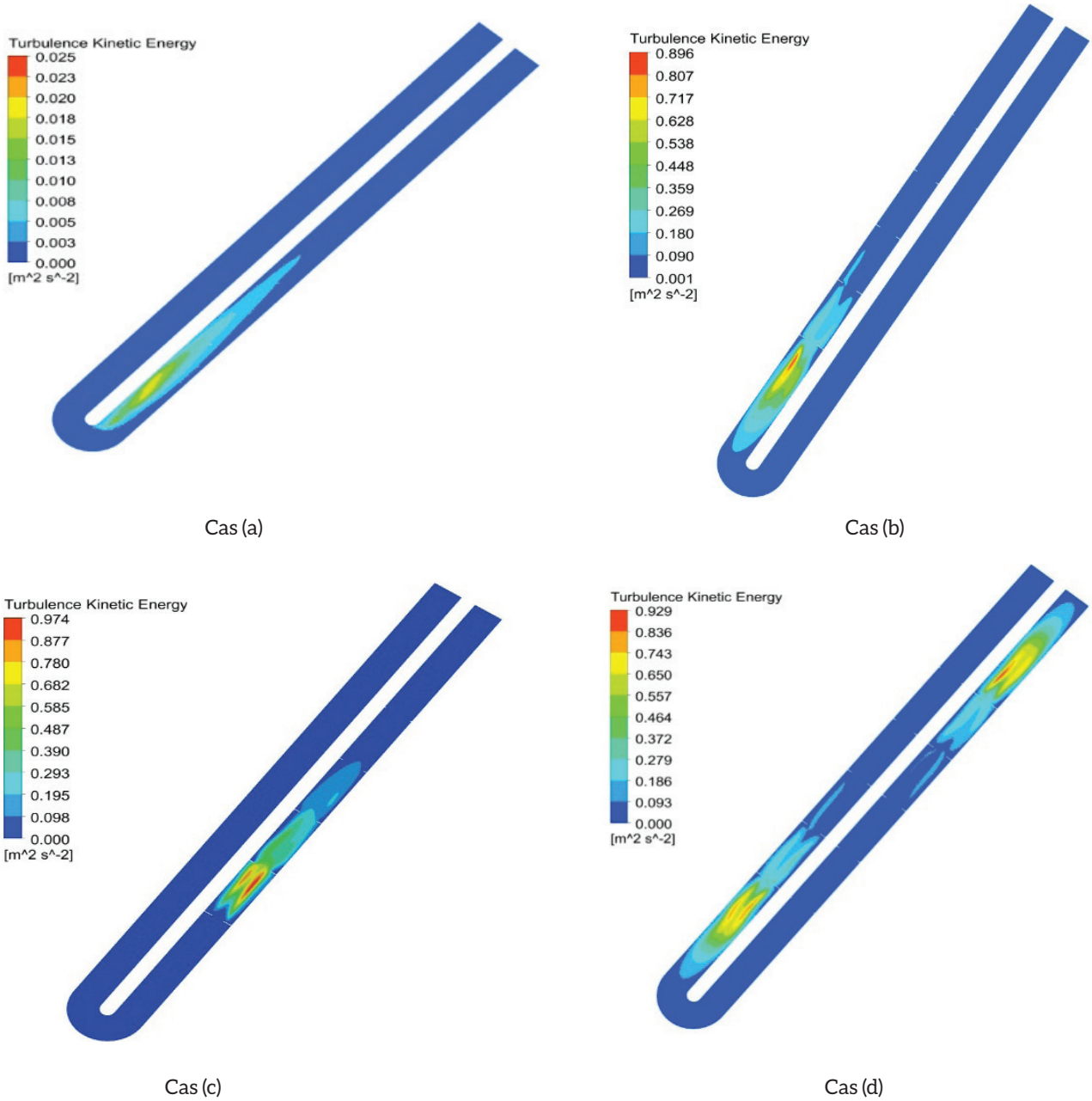

Fig. 8. 2D Contours of turbulence kinetic energy for different cases

Volume 11, Issue 1, June 2025 - ISSN 2356-8569
http://dx.doi.org/10.21622/RESD.2025.11.1.1150

The numerical results shown in Fig. 9 indicate that, initially, the fluid flow is well-organized, following parallel lines that suggest a regular, uniform displacement with minimal variation. However, upon interacting with the baffles, this smooth flow becomes disrupted. The baffles cause abrupt changes in both the velocity and direction of the fluid, breaking the uniformity of the initial laminar flow. This disturbance leads to the formation of vortices, characterized by rotational movements in the fluid. These vortices increase the turbulence, cause energy dissipation, and lead to localized fluctuations in temperature. The turbulence also affects the heat transfer efficiency, as these disturbances can create stagnant zones and irregular thermal exchanges. The more intense the turbulence, the more chaotic the flow becomes, diminishing the overall system performance in maintaining a consistent heat transfer rate.

This results in a higher thermal energy concentration at the outlet, improving the overall heat transfer rate. The turbulence generated by the baffles at the outlet enhances mixing, which not only increases the heat exchange efficiency but also contributes to better thermal performance in the system, as the fluid at the outlet is hotter compared to other regions. This configuration is beneficial for applications requiring more efficient heat extraction or distribution.

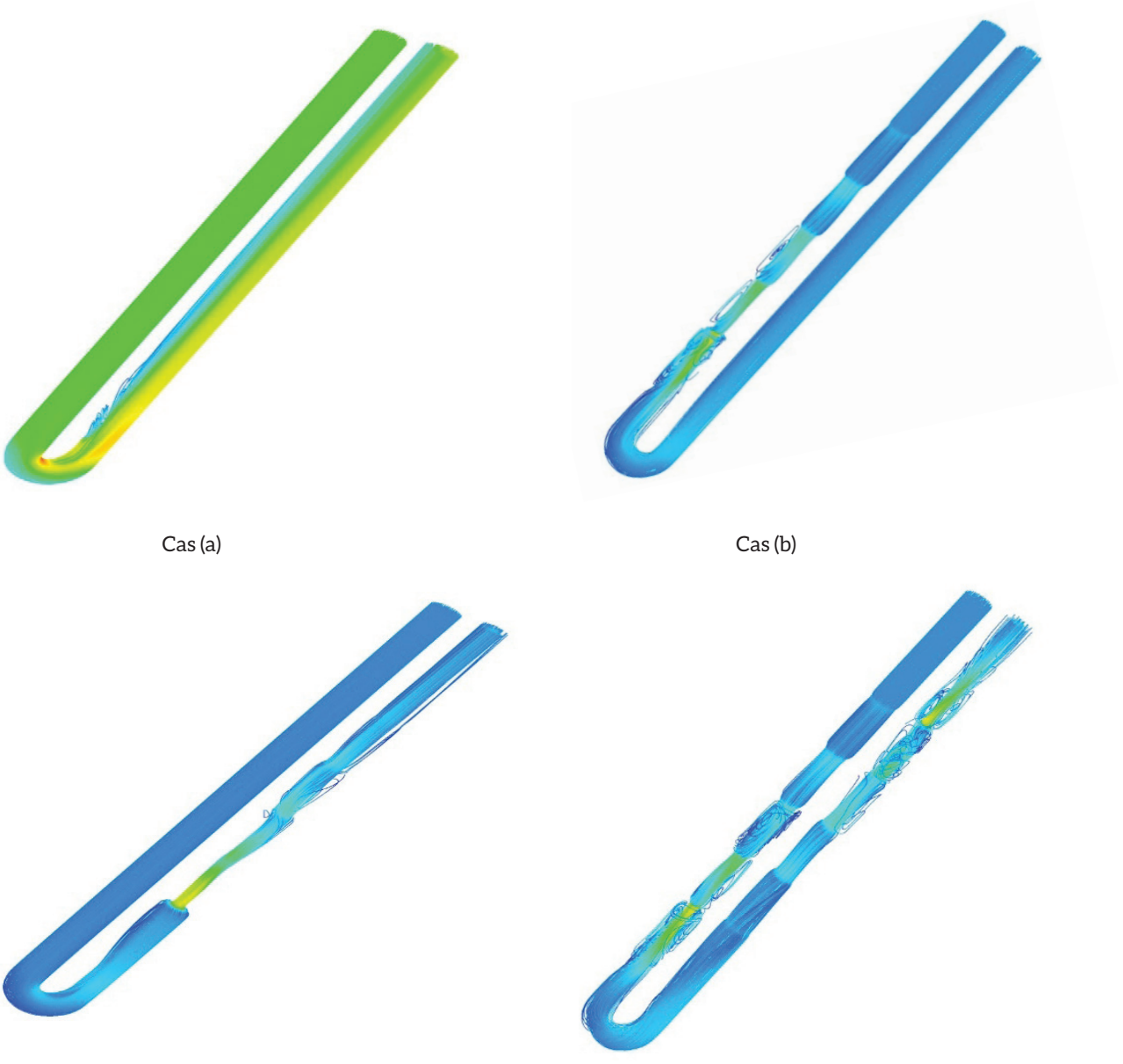

Fig. 9. 3D streamlines for different cases

Volume 11, Issue 1, June 2025 - ISSN 2356-8569
http://dx.doi.org/10.21622/RESD.2025.11.1.1150

Fig.10 shows the distribution of fluid temperature as a function of depth at the tube outlet for the four cases. It can be seen that:

- The temperature values at the outlet of the tube without baffles are low compared with the other cases with baffles.
- A significant variation in temperatures in the tube with baffles at the inlet compared with the tube with baffles at the outlet.
- A significant increase in fluid temperature in the tube with baffles (at the outlet, at the inlet and the tube without baffles) from - 0.8 m to 0 m depth.
- A very significant increase in fluid temperature in the tube with baffles at the outlet from -1 m to -0.8 m depth and a decrease from -0.8 m to -0.6 m compared with the other cases.
- At a depth of -1 m, the temperature of the fluid at the outlet of the tube with baffles at the inlet is higher, reaching 276.4 K, compared with the other cases.
- At a depth of 0 m, the temperature of the fluid in the outlet tube with baffles at the inlet and outlet is higher, reaching 279 K compared to the other cases.

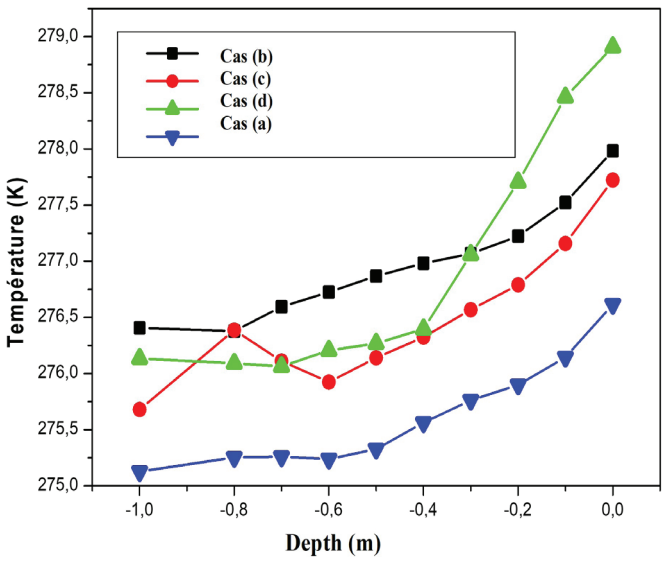

Fig. 10. Streamwise temperature profiles at the outlet of the pipe for different cases

Figures 11-14 show the fluid temperature distribution at the inlet and outlet of the U-tube as a function of depth, for the four cases studied: Case (a) an exchanger without baffles; case (b) an exchanger with perforated baffles of decreasing diameter in the inlet tube; case (c) an exchanger with perforated baffles of increasing diameter in the outlet tube; and the last case (d) an exchanger with perforated baffles in both the inlet and outlet tube. It can be seen that:

- The temperature of the fluid at the inlet remains constant at 275 K from 0 to 0.6 m for the four cases studied, then there is a slight increase in temperature from -0.6 m to -1 m depth; this increase increases with the addition of the baffles and is greater in case (d).
- The temperature of the fluid at the outlet increases significantly from 275.25 K to 276.75 K in case (a), 278 K in case (b), 277.5 K in case (c) and is highest in case (d) where the outlet temperature reaches its maximum value of 278.5 K.

This relative increase is due to convective heat transfer between the wall and the fluid, and to the use of baffles, which further improve heat transfer.

It can be seen that varying the internal diameter of the baffles has a strong influence on the increase in outlet temperature.

Case (d) where the baffles are placed on the outlet tube with decreasing baffle perforation diameters gives a better result than case (c) where the perforation diameters are increasing.

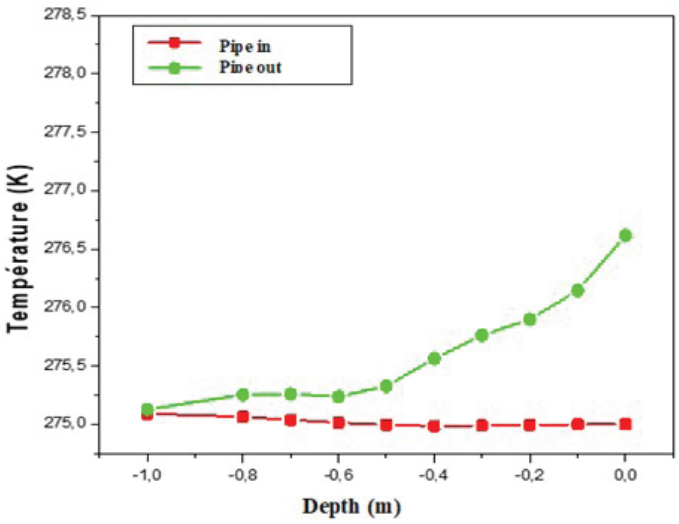

Fig. 11. Temperature profiles in case (a)

Volume 11, Issue 1, June 2025 - ISSN 2356-8569
http://dx.doi.org/10.21622/RESD.2025.11.1.1150

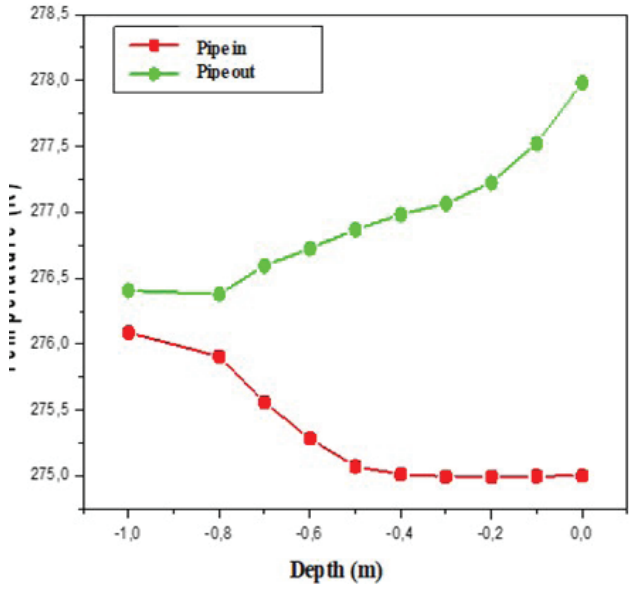

Fig. 12. Temperature profiles in case (b)

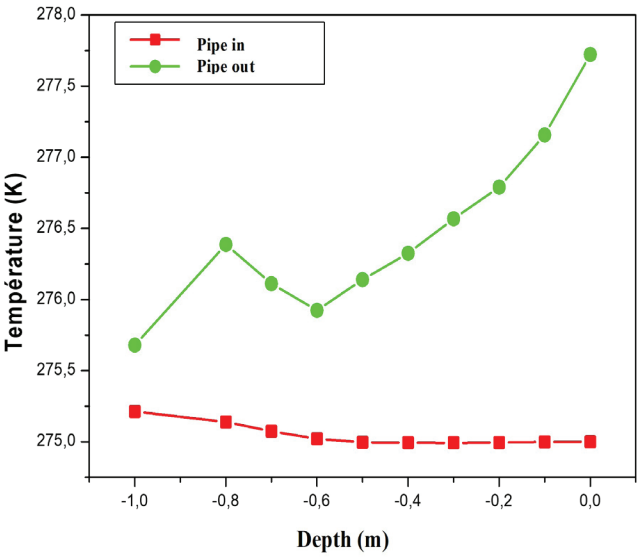

Fig. 13. Temperature profiles in case (c)

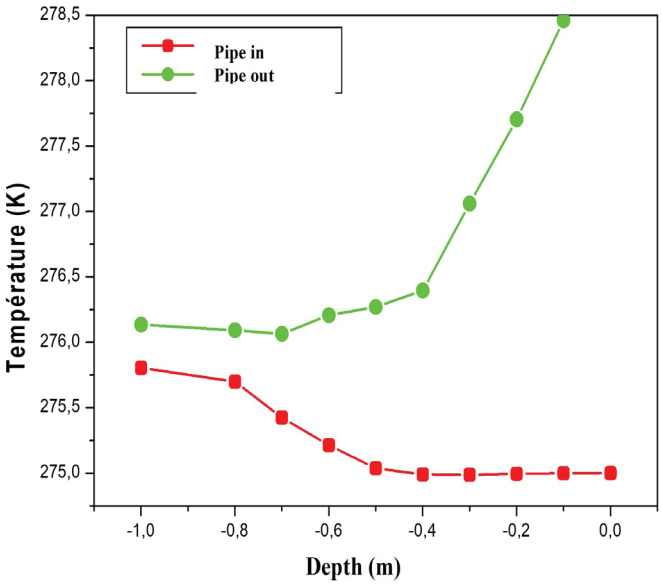

Fig. 14. Temperature profiles in case (d)

V. CONCLUSIONS

This 3D numerical study of a U-shaped tube with baffles provides a comprehensive analysis of how baffles influence both the dynamic flow characteristics and thermal performance within the heat exchanger. The results clearly demonstrate that the inclusion of baffles significantly improves heat transfer efficiency. Specifically, when baffles are positioned on both sides of the tube, the temperature difference between the inlet and outlet increases by 15%, highlighting enhanced thermal performance. The perforation diameter of the baffles is identified as a key factor in optimizing system performance. Smaller perforations at the outlet lead to a 12% increase in fluid temperature and more efficient energy utilization.

Volume 11, Issue 1, June 2025 - ISSN 2356-8569
http://dx.doi.org/10.21622/RESD.2025.11.1.1150

Among the configurations tested, case (d), where baffles are placed at the outlet with decreasing perforation diameters, outperforms case (c), which features increasing perforation diameters. Case (d) achieves a 20% improvement in heat transfer efficiency and a 10% increase in outlet temperature compared to the baseline configuration without baffles. These improvements result in superior energy savings and enhanced overall heating performance, making this configuration a promising solution for geothermal applications.

The study also provides deeper insights into the impact of baffle configurations on heat transfer, addressing key practical implications. For instance, the optimized baffle design enhances turbulence and fluid mixing, which are critical for improving thermal performance in real-world applications. This has direct relevance for industries relying on efficient heat exchange, such as geothermal energy production, HVAC systems, and industrial cooling processes. By maintaining a balance between heat transfer enhancement and pressure drop, the proposed design ensures minimal energy losses, making it economically and environmentally attractive.

For future research, it is recommended to explore various baffle materials and configurations to further enhance thermal efficiency. Additionally, investigating how different flow rates, fluid thermal properties, and baffle geometries influence system behavior would provide valuable insights into optimizing similar heat exchanger designs. Future work could also focus on examining the long-term performance and stability of such systems under varying operational conditions, as well as assessing the scalability of these findings for large-scale geothermal applications.

References

[1] J. Goldemberg *et al.*, "World energy assessment.".

[2] Thermal Use of the Underground; Part 1: Fundamentals, Approvals, Environmental Aspects. VDI-Richtlinien VDI 4640/I Verein Deutscher Ingenieure (VDI) in Düsseldorf, 2000.

[3] E. Abu-Nada *et al.*, "Modeling of a geothermal standing column well," *Int J Energy Res*, vol. 32, no. 4, 2008, doi: 10.1002/er.1355.

[4] A. Nguyen, P. Pasquier, and D. Marcotte, "Thermal resistance and capacity model for standing column wells operating under a bleed control," *Renew Energy*, vol. 76, 2015, doi: 10.1016/j.renene.2014.11.080.

[5] Dong Youp Kwak, Duhee Park, J. H. Chang, S. M. Na, and S. Park, "Parametric Study for Evaluation of Design Parameters of Standing Column Well," *Parametric Study for Evaluation of Design Parameters of Standing Column Well. In ProCeeding of World Geothermal COngreSS.*, 2010.

[6] D. Kim, M. Lim, B. Yu, and C. Lee, "Smart heating and cooling heat pump system by standing column well and cross-mixing balancing well heat exchangers," *Applied Sciences (Switzerland)*, vol. 10, no. 21, 2020, doi: 10.3390/app10217643.

[7] B. M. Ng, "Numerical Modeling of Multiple Standing Column Wells Applied to Geothermal Heating and Cooling in UK Buildings," Ph.D. Thesis, University of Northumbria at Newcastle., 2011. [Online]. Available: https://nrl.northumbria.ac.uk/id/eprint/7265/

[8] D. Pahud and B. Matthey, "Comparison of the thermal performance of double U-pipe borehole heat exchangers measured in situ," *Energy Build*, vol. 33, no. 5, pp. 503–507, May 2001, doi: 10.1016/S0378-7788(00)00106-7.

[9] J. A. Shonder and J. V. Beck, "Field test of a new method for determining soil formation thermal conductivity and borehole resistance," in *ASHRAE Transactions*, 2000.

[10] M. Inalli and H. Esen, "Experimental thermal performance evaluation of a horizontal ground-source heat pump system," Appl Therm Eng, vol. 24, no. 14–15, 2004, doi: 10.1016/j.applthermaleng.2004.01.005.

[11] M. Sheikholeslami, M. M. Rashidi, T. Hayat, and D. D. Ganji, "Free convection of magnetic nanofluid considering MFD viscosity effect," *J Mol Liq*, vol. 218, 2016, doi: 10.1016/j.molliq.2016.02.093.

[12] M. Sheikholeslami and D. D. Ganji, "Influence of electric field on Fe3O4- water nanofluid radiative and convective heat transfer in a permeable enclosure," *J Mol Liq*, vol. 250, 2018, doi: 10.1016/j.molliq.2017.12.028.

[13] M. Sheikholeslami, "Numerical simulation for solidification in a LHTESS by means of nano-enhanced PCM," *J Taiwan Inst Chem Eng*, vol. 86, 2018, doi: 10.1016/j.jtice.2018.03.013.

[14] G. Florides and S. Kalogirou, "Ground heat exchangers-A review of systems, models and applications," 2007. doi: 10.1016/j.renene.2006.12.014.

[15] H. Esen, M. Inalli, and M. Esen, "Numerical and experimental analysis of a horizontal ground-coupled heat pump system," *Build Environ*, vol. 42, no. 3, 2007, doi: 10.1016/j.buildenv.2005.11.027.

[16] M. Sheikholeslami, M. Jafaryar, D. D. Ganji, and Z. Li, "Exergy loss analysis for nanofluid forced convection heat transfer in a pipe with modified turbulators," *J Mol Liq*, vol. 262, 2018, doi: 10.1016/j.molliq.2018.04.077.

[17] K. S. Lee, "Modeling on the cyclic operation of standing column wells under regional groundwater flow," *Journal of Hydrodynamics*, vol. 23, no. 3, 2011, doi: 10.1016/S1001-6058(10)60116-3.

[18] E. Abu-Nada *et al.*, "Modeling of a geothermal standing column well," *Int J Energy Res*, vol. 32, no. 4, pp. 306–317, Mar. 2008, doi: 10.1002/er.1355.

[19] B. M. Ng, C. Underwood, and S. Walker, "Numerical modelling of multiple standing column wells for heating and cooling buildings," in *IBPSA 2009 - International Building Performance Simulation Association 2009*, 2009.

[20] B. M. Ng, C. P. Underwood, and S. L. Walker, "Standing column wells - Modeling the potential for applications in geothermal heating and cooling," *HVAC and R Research*, vol. 17, no. 6, 2011, doi: 10.1080/10789669.2011.588984.

[21] M. Haines and I. Taylor, "Numerical investigation of the flow field around low rise buildings due to a downburst event using large eddy simulation," *Journal of Wind Engineering and Industrial Aerodynamics*, vol. 172, 2018, doi: 10.1016/j.jweia.2017.10.028.

[22] Y. Hwang *et al.*, "Cooling performance of a vertical ground-coupled heat pump system installed in a school building," *Renew Energy*, vol. 34, no. 3, 2009, doi: 10.1016/j.renene.2008.05.042.

[23] R. Karabacak, E. Güven Acar, H. Kumsar, A. Gökgöz, M. Kaya, and Y. Tülek, "Experimental investigation of the cooling performance of a ground source heat pump system in Denizli, Turkey," *International Journal of Refrigeration*, vol. 34, no. 2, 2011, doi: 10.1016/j.ijrefrig.2010.10.009.

[24] O. Ozyurt and D. A. Ekinci, "Experimental study of vertical ground-source heat pump performance evaluation for cold climate in Turkey," *Appl Energy*, vol. 88, no. 4, 2011, doi: 10.1016/j.apenergy.2010.10.046.

[25] A. Michopoulos and N. Kyriakis, "Predicting the fluid temperature at the exit of the vertical ground heat exchangers," *Appl Energy*, vol. 86, no. 10, 2009, doi: 10.1016/j.apenergy.2009.02.002.

[26] A. Michopoulos, D. Bozis, P. Kikidis, K. Papakostas, and N. A. Kyriakis, "Three-years operation experience of a ground source heat pump system in Northern Greece," *Energy Build*, vol. 39, no. 3, 2007, doi: 10.1016/j.enbuild.2006.08.002.

[27] I. Kolo *et al.*, "A comprehensive review of deep borehole heat exchangers (DBHEs): subsurface modelling studies and applications," *Geothermal Energy*, vol. 12, no. 1, p. 19, Jun. 2024, doi: 10.1186/s40517-024-00297-3.

[28] Z. Ma *et al.*, "Effects of Boundary Conditions on Performance Prediction of Deep-Buried Ground Heat Exchangers for Geothermal Energy Utilization," *Energies (Basel)*, vol. 16, no. 13, p. 4874, Jun. 2023, doi: 10.3390/en16134874.

[29] L. Guo, X. Li, Z. Wang, Y. Ma, J. Zhang, and H. Jiang, "Investigation of heating potential and sustainability of medium-deep borehole heat exchanger in severe cold regions," Mar. 22, 2023. doi: 10.21203/rs.3.rs-2713296/v1.

[30] P. Zhang and B. Guo, "A Feasibility Assessment of Heat Energy Productivity of Geothermal Wells Converted from Oil/Gas Wells," *Sustainability (Switzerland)*, vol. 16, no. 2, 2024, doi: 10.3390/su16020768.

[31] S. Akbar, N. Fathianpour, and R. Al Khoury, "A finite element model for high enthalpy two-phase flow in geothermal wellbores," *Renew Energy*, vol. 94, pp. 223–236, Aug. 2016, doi: 10.1016/j.renene.2016.03.034.

[32] N. BniLam and R. Al-Khoury, "A spectral element model for nonhomogeneous heat flow in shallow geothermal systems," *Int J Heat Mass Transf*, vol. 104, pp. 703–717, Jan. 2017, doi: 10.1016/j.ijheatmasstransfer.2016.08.055.

[33] L. Benahmed and K. Aliane, "Simulation and Analysis of a Turbulent Flow Around a Three-Dimensional Obstacle," *Acta Mechanica et Automatica*, vol. 13, no. 3, pp. 173–180, Sep. 2019, doi: 10.2478/ama-2019-0023.

[34] L. BENAHMED, K. ALİANE, and A. J. CHAMKHA, "THREE-DIMENSIONAL SIMULATION OF A TURBULENT FLOW AROUND A TAPERED CUBE DUG IN THE MIDDLE," *Journal of Thermal Engineering*, vol. 7, no. 2, pp. 256–269, Feb. 2021, doi: 10.18186/thermal.872188.

[35] B. Rostane, K. Aliane, and S. Abboudi, "Three Dimensional Simulation for Turbulent Flow Around Prismatic Obstacle with Rounded Downstream Edge Using the k-ω SST Model," *International Review of Mechanical Engineering (IREME)*, vol. 9, no. 3, p. 266, May 2015, doi: 10.15866/ireme.v9i3.5719.

[36] B. Rostane and S. Abboudi, "Numerical Study of Laminar Fluid Flow Around Two Heated Wall-Mounted Perforated Cubes in Tandem Arrangement," *International Journal of Heat and Technology*, vol. 40, no. 1, pp. 157–166, Feb. 2022, doi: 10.18280/ijht.400119.

[37] S. Heinz, "From Two-Equation Turbulence Models to Minimal Error Resolving Simulation Methods for Complex Turbulent Flows," *Fluids*, vol. 7, no. 12, p. 368, Nov. 2022, doi: 10.3390/fluids7120368.

[38] B. Cui, X. Wang, R. Wang, and Z. Xiao, "Numerical investigation of transonic axial compressor rotor flows using an improved transition-sensitized turbulence model," *Physics of Fluids*, vol. 33, no. 3, Mar. 2021, doi: 10.1063/5.0043633.

[39] X. Wang, B. Cui, and Z. Xiao, "Numerical investigation on ultra-high-lift low-pressure turbine cascade aerodynamics at low Reynolds numbers using transition-based turbulence models," *Journal of Turbulence*, vol. 22, no. 2, 2021, doi: 10.1080/14685248.2020.1849712.

[40] P. Jalili, D. D. Ganji, and S. S. Nourazar, "Investigation of convective-conductive heat transfer in geothermal system," *Results Phys*, vol. 10, 2018, doi: 10.1016/j.rinp.2018.06.047.

[41] R. Al-Khoury, *Computational Modeling of Shallow Geothermal Systems*. 2011. doi: 10.1201/b11462.